Металлофиз. новейшие технол. / Metallofiz. Noveishie Tekhnol.
2013, т. 35, № 2, сс. 241–252
Оттиски доступны непосредственно от издателя
Фотокопирование разрешено только
в соответствии с лицензией

PACS numbers: 06.60.Vz, 62.20.fq, 62.20.Qp, 81.20.Vj, 81.40.Lm, 81.40.Pq, 82.80.-d

Effect of Friction Time on Microstructure and Mechanical Properties of Friction Welded AISI 304 Stainless Steel to AISI 1060 Steel

Hakan Ates and Nihat Kaya*

Gazi University,
Faculty of Technology,
06500 Ankara, Turkey
**Gazi University,*
Institute of Science and Technology,
06500 Ankara, Turkey

The influence of friction time on the hardness, tensile properties, and microstructure of the welded samples is investigated. With increasing friction time, the hardness and tensile strength values increase too. The hardness of the welding interfaces is higher than that of the base alloys. Microstructures of the welds are examined by the optical and scanning electron microscopy. The results show that all welding joints are perfectly bonded and free of any cracks, pores, and defects. The tensile fracture of welded joint occurred in the AISI 304 side. The chemical composition of the interfaces and deformation zones are detected using energy dispersive spectroscopy. Diffusion of the Cr and Ni is evident on the AISI 1060 side.

Досліджено вплив тривалости тертя на твердість, властивості при розтягу та на мікроструктуру зварних зразків. При збільшенні тривалости тертя твердість та границя міцности на розрив також збільшуються. Міцність поверхні зварних контактів виявляється більшою, аніж у основних стопів. Мікроструктуру зварних швів було досліджено методами оптичної й електронної мікроскопії. Показано, що зварні з'єднання були досконало звареними та не мали ніяких тріщин, пор і дефектів. Руйнування при розтягу відбувалося з боку криці AISI 304. Хемічний склад зварних контактів і зон деформації досліджено за допомогою енергодисперсійної спектроскопії. Спостерігалася дифузія Cr та Ni в бік криці AISI 1060.

Исследуется влияние времени трения на твёрдость, свойства при растяжении и на микроструктуру сварных образцов. При увеличении времени трения твёрдость и предел прочности на разрыв также увеличиваются. Прочность поверхности сварных контактов оказывается выше, чем у основных сплавов. Микроструктура сварных швов исследуется методами

оптической и электронной микроскопии. Показано, что все сварные соединения были идеально сварены и не имели никаких трещин, пор и дефектов. Разрушение при растяжении происходит со стороны стали AISI 304. Химический состав сварных контактов и зон деформации исследуются с помощью энергодисперсионной спектроскопии. Наблюдается диффузия Cr и Ni в сторону стали AISI 1060.

Key words: AISI 304 SS–AISI 1060, friction welding, microstructure, mechanical properties.

(Received December 29, 2011; in final version, February 12, 2013)

1. INTRODUCTION

Austenitic stainless steels based on relatively high amount of Cr and Ni are excellent candidates to be used as structural materials in chemical and food industry as well as in hospital surgical equipments. They exhibit high ductility, excellent drawing and forming properties. The various fusion and solid state welding techniques can be used to join these steels. Welding of machinery parts is necessary in the most of the engineering applications. Just a few decades ago, materials were classified as weldable and non-weldable, but innovations in technology enabled the joining of majority of materials by fusion and solid state welding techniques. Some of the fusion techniques are applied for various materials [1–3]. The typical solid-state joining applications of diffusion welding for various content of the aluminium metal matrix composites [4] and FSW [5] have been studied in detail. Welding time, applied load, welding temperature and chemical composition of the steel are some of the key parameters to control solid-state diffusion welding process.

Rotary friction welding is one of the solid state joining techniques, which is applied to join similar and dissimilar counterparts. In this technique, machinery components are brought into contact with one another. While one of them remains stationary, the other is rotated with the applied pressure. When the temperature of the interfaces has reached an optimum value for the extensive plastic deformation, the rotation is stopped, while the forging pressure remains unchanged or increased. The application of an axial force maintains intimate contact between the parts and leads to plastic deformation in the material near the weld interface. If sufficient frictional heat has been produced during softening, larger wear particles begin to expel from the interfaces, and axial shortening of the components begins as a result of the expelled upsetting. In general, heat is conducted away from the interfaces, and plastic zone develops. The plasticized layer is formed on the interfaces and the local stress system with the assistance of the rotary movement extrudes material from the interface into the flash. It is

shown that the weld integrity is strongly affected by the rate of flash expelled under the appropriate conditions [6]. Friction welding has a lot of advantages over other welding processes. Among these advantages are no melting, high reproducibility, short production time, low energy input, limited heat affected zone (HAZ), avoidance of porosity formation and grain growth and the use of non-shielding gases during welding process. In addition, the technique is not only applied to round specimens but is also used for rectangular components. It is called linear friction welding and has recently been applied to the steel [7].

Although a large amount of previous studies [4–11] in similar and dissimilar materials have been studied, mechanical properties of the plain carbon steel to stainless steel joint by friction welding method have never been reported up to date. Therefore, in this paper, the AISI 1060 and AISI 404 stainless steel are welded by friction welding and the mechanical, microstructural properties and optimal welding conditions of friction welded samples are examined.

2. MATERIALS AND METHODS

Chemical composition of plain carbon steel and stainless steel employed is presented in Table. Cylindrical test specimens of 20 mm in diameter and 160 mm in the length were prepared for friction welding. Before the friction welding, the surfaces facing each other were machined using a lathe. Before welding, the surfaces of the work pieces were cleaned by a stainless steel brush and acetone to remove the oxide layer and stains. Joining of these two dissimilar alloys was performed on a continuous drive friction-welding machine of 300 kN capacity at a constant rotation speed of 2000 rpm, and constant friction pressure (P_1) of 40 MPa and constant upsetting pressure (P_2) of 60 MPa. Friction and upsetting pressures can be observed on the screen, and the stages of welding sequence are controlled by solenoid valve. The friction time (t) was chosen as three, five, and seven seconds. Tensile test specimens were prepared according to ASTM E8M-00b. Ultimate Tensile Strength (UTS) and yield strength of the welded specimens were determined. Hardness values (VH_1) were determined using Shimadzu

TABLE. Chemical composition of tested materials.

Material	C	Cr	Ni	Si	Mn	P
AISI 1060	0.42	–	–	0.21	0.45	0.02
			Elements, wt.%			
Material	C	Cr	Ni	Si	Mn	P
AISI 304	0.027	8.1	18.1	0.28	1.81	0.073

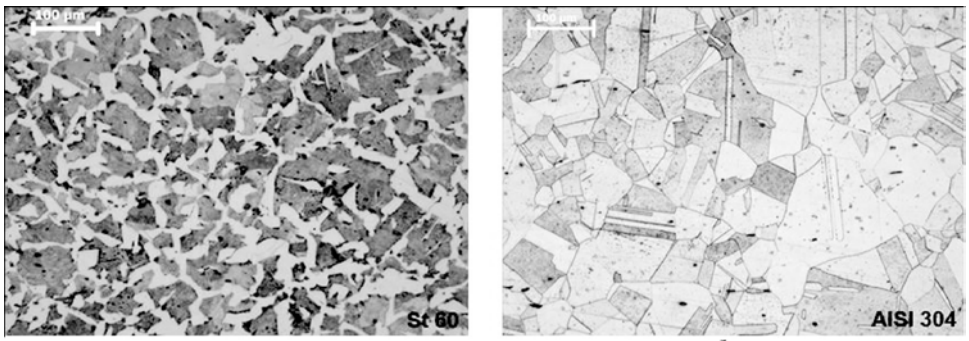

a *b*

Fig. 1. Microstructure of AISI 1060 (*a*) and AISI 304 (*b*).

HMV device. Measurements were taken in the welding centre through base metal with a distance of 1 mm on either side of horizontal line. Hardness values were measured in the welding centre through the diameter with a distance of 2.5 mm on vertical line. For tensile strength and hardness test values, at least, three specimens were prepared for each parameter. The microstructure was investigated with the SEM and optical microscopy. The AISI 1060 steel specimens were polished and etched with a solution consisting of 4% Nital. AISI 304 SS etched with a solution of 95% HCl and 5% $OH{-}C_6H_2(NO_2)_3$. The grains have various shapes ranging from 10 μm to 300 μm in dimension. Typical microstructures of materials can be seen in Fig. 1.

3. RESULTS AND DISCUSSIONS

3.1. Hardness Distribution

Figure 2, *a* shows the effect of friction time on the hardness distribution in the direction perpendicular to the weld interface of the as-welded specimen. The maximum hardness values of joints were obtained on the welding centre line. The hardness values generally increased with friction time. Increasing hardness in the welding interface can be related to the microstructure formed in the joint surface as a result of the heat input and extensive plastic deformation. The hardness of AISI 304 SS is 129 *HV* and the hardness value of the AISI 1060 steel is 254 *HV*, but measured hardness of welding interface is around 300 *HV*. We can suppose that microstructural evaluations around the interface, diffusion of elements on the sides, work hardening, dislocation density, grain refinement, and formation of precipitations may cause this increase. Although the work hardening is effective on the SS side, phase transformation, fine grains and formation of precipitates

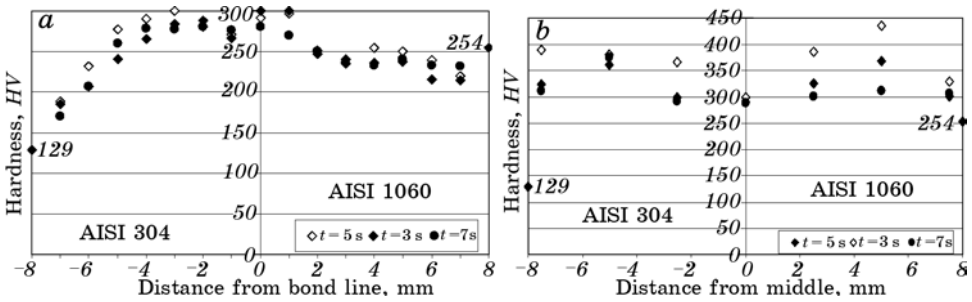

Fig. 2. The effect of friction time on horizontal (*a*) and vertical (*b*) hardness distribution.

and rapid cooling from the welding temperature resulted in the hardening in the AISI 1060 steel. Similar hardness profile was also observed for dissimilar materials couples [11]. One can suppose that the hardness properties are influenced by an interactive effect of friction time, which is combinations of heat input, range of plastic deformation and degree of strain hardening. The influence of the friction time on the vertical hardness distribution is also shown in Fig. 2, *b*. Both sides of materials are hardened due to the austenite transformation to the martensite formation, which is strongly affected by the cooling rate. All hardness values are higher than those in the base metal are. It was observed that hardness values increased from the centre through the thickness of the specimen. The phase transformation and cooling rates were the optimum around 5 mm away from the centre.

3.2. Tensile Properties

The influence of friction time on the tensile test result is shown in Fig. 3. It can be seen that the yield strength slightly increased with the in-

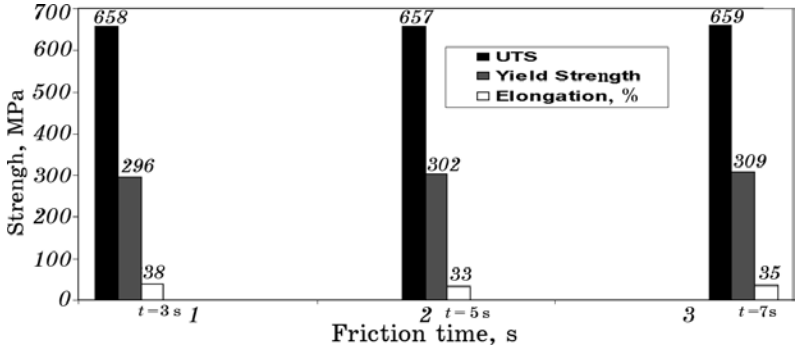

Fig. 3. The effect of friction time on the tensile properties.

crease of friction time. The UTS value for the AISI 1060 is 814 MPa and for the AISI 304 SS it is 505 MPa [12]. The UTS strength corresponds to about 130% of that for AISI 304 SS part and 81% of that for AISI 1060 structural steel part. Although the UTS values were not influenced by friction time, the highest yield strength is obtained with the highest friction time.

Fabricated joints were quite ductile in nature and 3 s and 5 s samples failed in the AISI 1060 side due to the low elongation, which is only 17% compared to 70% for the SS. However, when the friction time increased to the 7 s, failure occurred on the SS side (see Fig. 4) due to the extended deformation and heat affected zone. Almost all specimens failed on the base metals, showing that perfect joint interfaces were obtained under the various friction times. It is reported that the choice of welding parameters affects the microstructure [13–15]. If the friction time is held long, a broad diffusion zone with intermetallic phases may be generated. Such parameters as short friction time, low friction and low upsetting pressures will result in a weakly bonded joint. Hence, the quality of the welds strongly depends on the temperature attained by each substrate during welding process. Therefore, the flow stress–temperature relationship for each metal will have an important influence on the friction welding parameters. However, it is also reported that a good strength can be obtained by a sufficient diffusion and mechanical locking [11]. If optimum welding parameters are used in friction welding, a perfect bonding can be achieved. In general, high friction and upsetting pressures resulted in high toughness and hardness in steel alloys [8]. It is also well known that for achieving high strength at welding interface the brittle phases such as σ-phase, δ-ferrite and oxide formations should be pushed away from the joint surface. In this case, to achieve higher strength, the friction and upsetting pressures should be as high as possible for the constant friction time. As the friction and wear help to get rid of contaminants like oxide on the interface, a new face should be surfaced. At the same time, the upsetting and friction pressure and friction time set in to bring the new face within the scope of attraction range [14, 15].

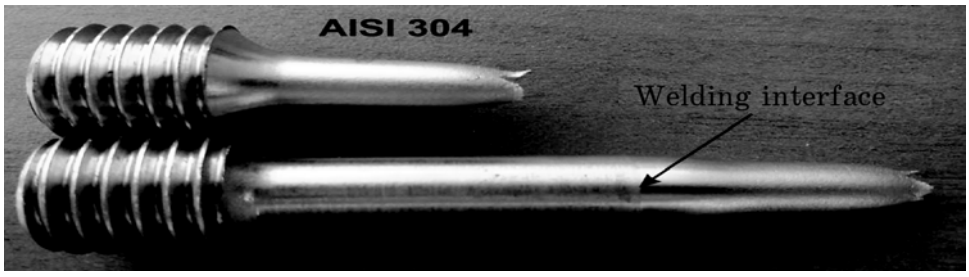

Fig. 4. Tensile test sample macrograph of fractured surface.

3.3. Microstructure

Figure 5 shows the typical microstructural features of the welded samples. As seen from the macrographs, flash formation was observed in all welded samples because of plastic deformation during welding. Friction

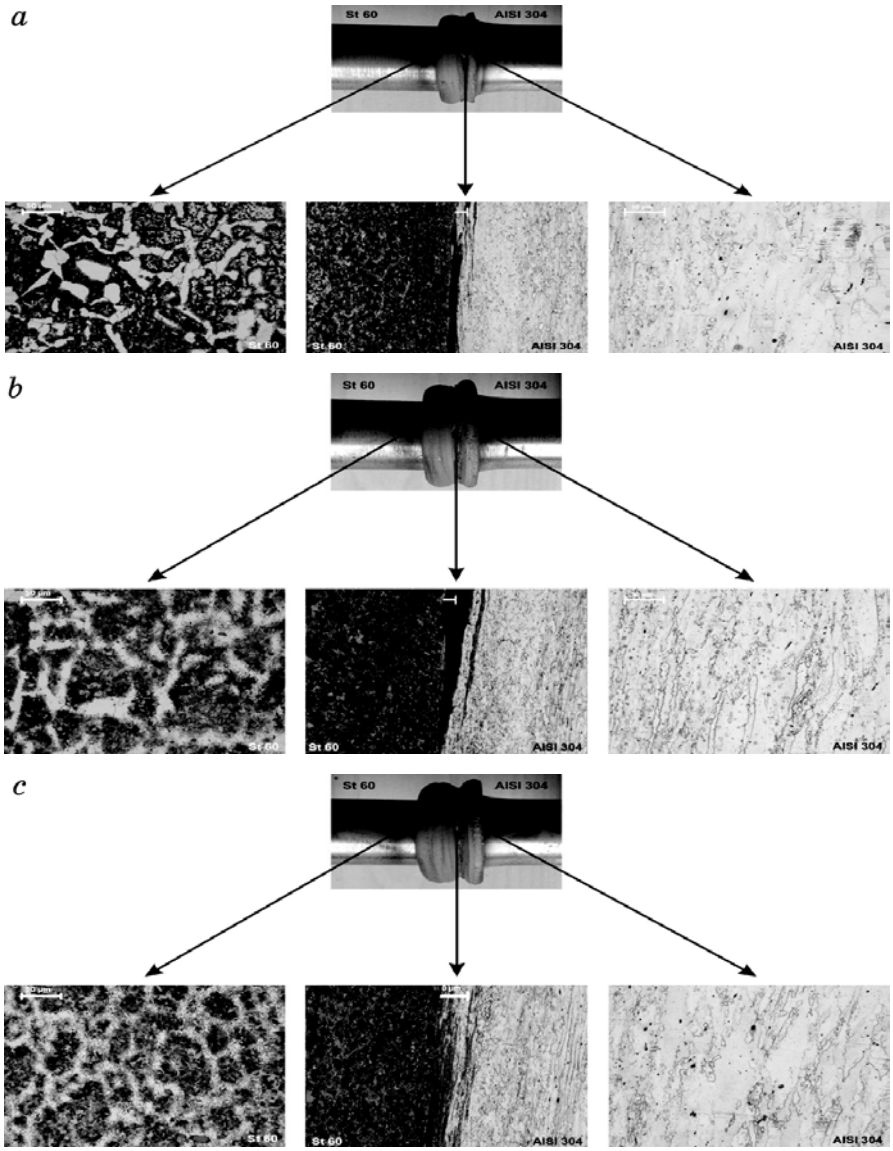

Fig. 5. Typical macro- and microstructure of the friction welding parts; P_1 = = 40 MPa, P_2 = 60 MPa, t = 3 s (*a*), 5 s (*b*), 7 s (*c*).

time plays an important role in flash formation, which gets bigger with increasing friction time on both sides of materials due to the higher heat input and extensive plastic deformation. Thus, the burn-off (axial shortening) increases with the increase of plastic deformation (see Figs 5, *a*, *c*). All of the welded joints were perfectly bonded and free of any crack, pore and defect.

Two main regions are observed on the welded samples: a dynamically recrystallized zone with extremely fine grains and plastically deformed heat affected zone (see Figs. 6, *a*–*c*). The width of both zones changes due to the materials properties, *i.e.* yield strength, coefficient of thermal expansion (CTE), and ductility. Low yield strength, high heat conductivity and high ductility at elevated temperatures causes more deformation of the AISI 1060 side compared with AISI 304 side. Thus, deformation that is more plastic, extended HAZ and more axial shortening were observed on AISI 1060 side and these properties expanded with increased friction time. Figures 6, *a*–*c* also show the grain orientation inside the HAZ zones. The intensity of orientation depends on the welding parameters [11]. It is clearly seen that sufficient friction time on the joining surface resulted in an adequate locking of the surfaces, where extensive plastic deformation and microstructural changes occurred, and these facts

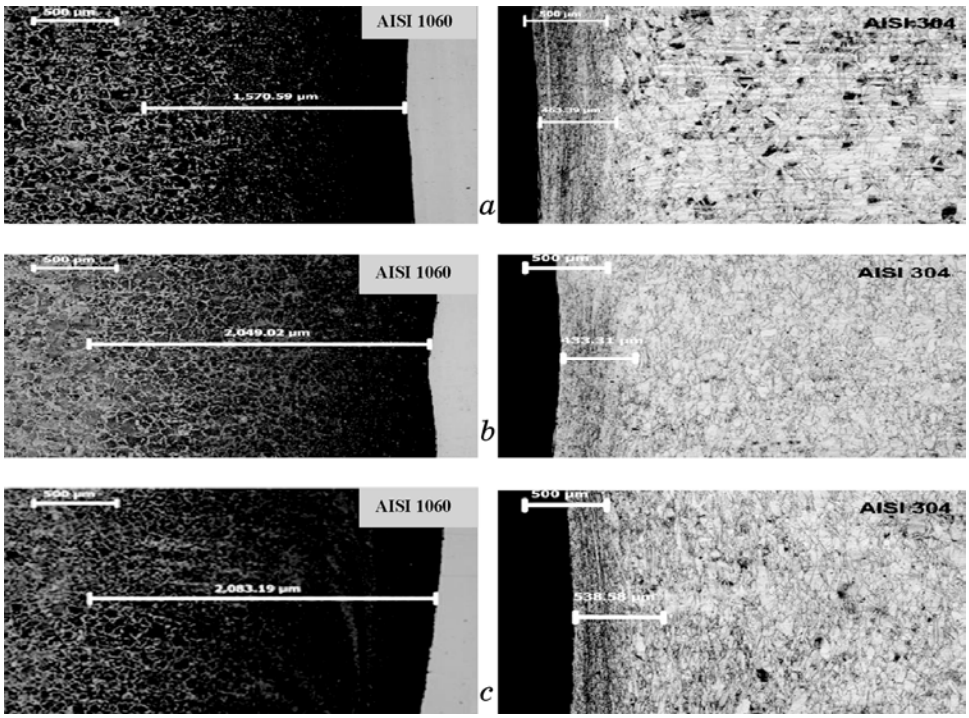

Fig. 6. The effect of friction time on deformation zone: 3 s (*a*), 5 s (*b*), 7 s (*c*).

caused better tensile response of the joint, where recrystallization occurred on the AISI 1060 side (higher deformation) and grain refinement and strain hardening occurred on the AISI 304 steel side (lower deformation). The width of recrystallized zone is mainly affected by the friction time. An increase in the friction time results in wider size of fine grain region. The change of microstructure and higher axial shortening is also observed in the AISI 1060 side.

Heat flow is observed preferentially in the material with the higher thermal conductivity. Due to the different thermal conductivities of AISI 304 (16.2 $W \cdot m^{-1} \cdot K^{-1}$) and AISI 1060 (49.8 $W \cdot m^{-1} \cdot K^{-1}$), the specific heat was so large, and hence most of the frictional heat generated in the AISI 1060 side. The difference in thermal conductivity explains the microstructural changes, which occur preferentially in the AISI 1060 side. Similar microstructural observations for the Cu–Ti couples were also reported in [16]. Most of the changes took place in the copper, no evidence of microstructural variation was seen in the vicinity of the interface, and neither grain growth nor grain boundary precipitation was observed. This behaviour can be attributed to the difference of thermal conductivity [16].

Figures 5 and 6 also show the microstructural changes of AISI 304 side and AISI 1060 side of weld. During the friction welding process, the temperature near the welding interface reaches just above A_1 temperature, which is almost equal to the recrystallization temperature for the steel. Therefore, extremely fine equiaxed grains formed from ferrite and pearlite. Martensitic structure could also be seen in this region, when the welding interface reaches A_3 temperature with the occurrence of rapid cooling. Therefore, the microstructure of AISI 1060 steel turned into austenite. When austenitic structure was exposed to top cooling from evaluated temperatures, the microstructure turned into martensite due to the diffusion of carbon to the grain boundary and rapid cooling rate. These results mean that the weld experienced different thermal histories. The relatively quick cooling rate influenced the microstructure of the weld.

Figures 7 (1) and (2) show energy dispersive spectroscopy (EDS) analysis points observed on the AISI 304 side, while (4) and (5) show EDS analysis points observed on the AISI 1060 side. It is seen that alloying element concentration significantly changed at the joint surface (Point 3) and adjacent to the Point 3 due to the mechanical locking and atomic diffusion. In the joint surface Cr (1.53%) was measured for 3 s friction time. However, the increase of the friction time caused high density of Cr in the surface, where more heat generated as a result of high friction pressure. It is obvious that Cr atoms with smaller diameter are more mobile and diffusive inside this region. Significantly high amounts of Cr and Ni are detected on the AISI 1060 side in Point (4) and (5) under all conditions. Çelikyürek et al. [17] have reported the same phenomenon for Fe–28Al and 316 L SS.

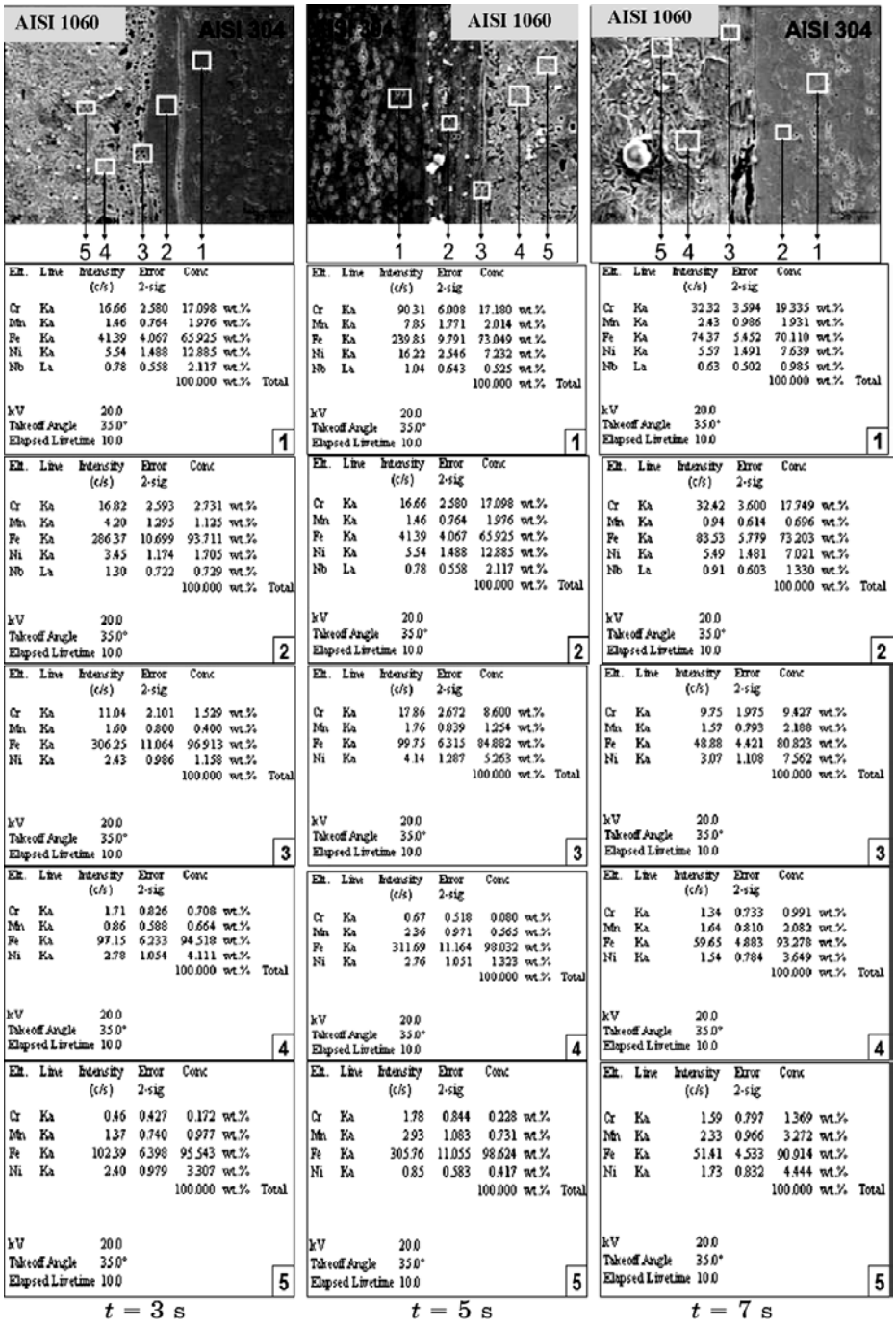

Fig. 7. Joint surfaces and location of the EDS analysis sites. The effect of friction time on the elemental distribution.

High amount of Al, Cr, and Ni atoms were diffused into interface and HAZ region due to the long period of friction time.

4. CONCLUSIONS

Based on the results obtained in this study, the following conclusions could be drawn.

1. Friction welding can be used successfully to join austenitic stainless steel (AISI 304) to AISI 1060 structural steel. The processed joints exhibited better mechanical and metallurgical characteristics.
2. The highest hardness values were observed in the interface, but they significantly varied with increasing distance and friction time. The increase in the hardness at the joint zone may be attributed to the microstructural evaluation.
3. The tensile strength of friction-welded joints was not affected by friction time. The tensile strength of obtained weld joints can exceed AISI 304 SS strength by 30%. Fracture usually occurs in the HAZ of AISI 1060 steel side.
4. An extensive deformation occurred mostly to the AISI 1060 side due to its flow stress and high thermal conductivity.
5. Typical microstructural features were observed in the welding region. Recrystallized fine and elongated grains were observed near the joint surface. The width of recrystallized region is mainly affected by the friction time.
6. The variance in weight of alloying elements is seen from analysis of elements spectra. EDS measurements clearly show that steel joints consist of different crystal structure, carbides and intermetallic compounds. Diffusion of the Cr and Ni is observed in the AISI 1060 side.

ACKNOWLEDGEMENTS

The authors wish to thank Prof. Dr. A. Kurt, Prof. Dr. N. Kahraman and Prof. Dr. I. Uygur for their invaluable contribution. Also special thanks to Turkish Track Factory for their support and guidance during the experimental stage.

REFERENCES

1. I. Uygur and B. Gulenc, *Metallurgiya*, **43**, No. 1: 35 (2004).
2. I. Uygur, *Industrial Lubrication and Tribology*, **58**, No. 6: 303 (2006).
3. I. Uygur and I. Dogan, *Metallurgiya*, **44**, No. 2: 119 (2005).
4. I. Uygur, *Mater. Sci. Forum*, **546–549**: 671 (2007).
5. A. Kurt, I. Uygur, and H. Ates, *Mater. Sci. Forum*, **534–536**: 789 (2007).
6. A. Vairis and M. Frost, *Mater. Sci. Eng. A*, **271**: 477 (1999).

7. W. Y. Li, T. J. Ma, S. Q. Yang, Q. Z. Xu, Y. Zhang, J. L. Li, and H. L. Liao, *Mater. Lett.*, **62**: 293 (2008).
8. P. Sathiya, S. Aravidan, and A. Noorul Haq, *Int. J. Adv. Manufac. Technol.*, **31**: 1076 (2007).
9. S. D. Meshram, T. Mohandas, and G. M. Reddy, *J. Mater. Proces. Techn.*, **184**: 330 (2007).
10. K. Jayabharath, M. Ashfaq, P. Veugopal, and D. R. G. Achar, *Mater. Sci. Eng. A*, **454**: 114 (2007).
11. N. Ozdemir, F. Sarsilmaz, and A. Hascalik, *Mater. Design*, **28**: 301 (2007).
12. www.matweb.com
13. A. Kurt, I. Uygur, and U. Paylasan, *Welding Journal*, **90**: 102 (2011).
14. H. Ates, M. Turker, and A. Kurt, *Mater. Design*, **28**: 948 (2007).
15. M. Sahin, H. E. Akata, and K. Ozel, *Mater. Design*, **29**, No. 1: 265 (2008).
16. S. Y. Kim, S. B. Jung, and C. C. Shur, *J. Mater. Sci.*, **38**: 1281 (2003).
17. I. Çelikyürek, O. Torun, and B. Baksan, *Mater. Sci. Eng. A*, **528**: 8530 (2011).